4 Sample Rotation

4.1 Spinning Around One Fixed Axis

"Nuclear magnetic resonance spectra from a crystal rotated at high speed" was the title of the first MAS paper by Andrew *et al.* [1] in 1958; see also [2]. The rotation frequency was 1.66 kHz, and an external magnetic field of 0.6 T was applied [1]. Fields of more than 20 T and MAS frequencies above 100 kHz are now available, but the basic theory has not changed.

The common definition for the magic-angle θ_m between the axis of rotation and the external magnetic field is $(3\cos^2\theta_\mathrm{m} - 1) = 0$. The angular dependence in the brackets corresponds to the term $m' = m = 0$ in the table of the Wigner D-Matrix elements for rank k = 2; see Table 1.1. Therefore, θ_m plays the role of a magic angle only for those interactions that can be described by a second-rank tensor like homonuclear and heteronuclear dipolar interactions, chemical shift anisotropy, first-order quadrupole interactions, and inhomogeneities of magnetic susceptibility.

We consider the term rank $k = 2, q = 0$, in the laboratory axis system (LAB) for dipolar interaction, chemical shift anisotropy or first-order quadrupole interaction (see Section 1):

$$\mathcal{H}_\mathrm{D,CSA,Q} \sim T_0^{(2)} V_0^{(2)\,\mathrm{LAB}}. \tag{4.01}$$

The sample rotation with the angular frequency ω_ROT about an axis, which is inclined by the angle θ with respect to the external magnetic field, requires the transformation

$$V_0^{(2)\,\mathrm{LAB}} = \sum_{q=-2}^{+2} V_q^{(2)\,\mathrm{ROT}} \exp(\mathrm{i}\omega_\mathrm{rot}\, q\, t)\, d_{q\,0}^{(2)}(\theta). \tag{4.02}$$

The operator components $V_q^{(2)\,\mathrm{ROT}}$ refer to the rotor axis system (ROT), which rotates in synch with the rotor in the LAB.

Eq. (4.02) includes the reduced real Wigner matrix elements (see Table 1.1),

$$d_{0\,0}^{(2)} = \frac{1}{2}\,(3\cos^2\theta - 1), \qquad d_{\pm1\,0}^{(2)} = \mp\sqrt{\frac{3}{2}}\sin\theta\cos\theta, \quad d_{\pm2\,0}^{(2)} = \sqrt{\frac{3}{8}}\sin^2\theta. \tag{4.03}$$

Eq. (4.02) describes with $q = 0$ the centerband and with $q = 1$ and $q = 2$ the spinning sidebands at multiples of ω_rot and $2\omega_\mathrm{rot}$, respectively. Spinning sidebands do not occur if the rotation frequency is large compared to the width of the static spectrum.

The element $q = 0$ in Eq. (4.02) describes the time-independent (or time-averaged) part of the tensor:

$$\overline{V_0^{(2)\,\mathrm{LAB}}} = \frac{1}{2}\,(3\cos^2\theta - 1)\, V_0^{(2)\,\mathrm{ROT}}. \tag{4.04}$$

We have $\overline{V_0^{(2)\,\mathrm{LAB}}} = V_0^{(2)\,\mathrm{ROT}}$ for $\theta = 0°$, and $\overline{V_0^{(2)\,\mathrm{LAB}}}$ becomes zero for $\theta = \theta_\mathrm{m}$. In the following we consider the case $\theta \cong \theta_\mathrm{m}$. The factor on the right-hand side of Eq. (4.04) is the scaling factor of a signal broadened exclusively by second-rank interactions. If we aim for a resolution of 100 Hz, and the static width of the spectrum is 10 kHz, this factor should be smaller than 1/100. This corresponds to $|\theta - \theta_\mathrm{m}| < 0.4°$. But the adjustment has to be even better for ST MAS NMR (see Section 6), or for ^{2}H MAS NMR spectroscopy of solids. The latter faces a static line width of about 200 kHz, requiring

that $|\theta - \theta_\mathrm{m}| < 0.02°$. ST MAS demands even more precise conditions, $|\theta - \theta_\mathrm{m}| < 0.002°$ [3-5], due to larger quadrupole broadenings. The usual mechanism for setting the magic angle is hardly sufficient for such precision. Mamone *et al.* [6] proposed a Hall sensor affixed to the MAS stator in order to achieve a precision of about $0.01°$.

The first-order quadrupole interaction can be viewed as an inhomogeneous interaction [7], and each satellite transition behaves exactly the same as a chemical shift anisotropy. The central transition has no orientation dependence in the first order and is thus unaffected by MAS. Spinning sidebands appear around the Larmor frequency ν_L at $\nu_\mathrm{L} + n\,\nu_\mathrm{rot}$, where $|n| = 1, 2, 3, \ldots$ is limited by the static line width. The line at ν_L is usually called the "centerband". Hence, for quadrupole nuclei the centerband is the sum of the $2I - 1$ centerbands of the satellite transitions and the central transition. The centerbands due to the satellite transitions must not be confused with the central transition. If the central transition is broadened by other interactions, it may also split into a centerband and various spinning sidebands. In the time-domain the satellite transitions appear as rotational echoes at times $t = n/\nu_\mathrm{rot}$. For a total of N spinning sidebands in the frequency domain, the echoes in the time-domain are a superposition of N cosine functions, $\cos(2\pi n \nu_\mathrm{rot} t)$. The envelope of the echo train is given by the inverse line width of a single MAS line. The magnitude of such a single echo is proportional to the total number of sidebands, N, and its width is proportional to $1/N$. Therefore, maximizing the magnitude of an echo after the Fourier transform maximizes the number of observed spinning sidebands, and the first-order quadrupole interaction may be used to set the magic angle [8].

The first-order quadrupole broadening is typically larger than the MAS rotation frequency. Thus, the envelope of the first-order MAS powder pattern can be used to determine the quadrupole parameters, if the whole spectrum can be excited and the MAS rotation frequency is large compared to the second-order broadening. The signal-to-noise ratio of the MAS spectrum is higher than that of the static spectrum, since the area under the line shape function is not changed upon MAS. Therefore, quadrupole parameters and chemical shifts can be determined using a high-performance broadband MAS probe [9-12].

Second-order quadrupole interaction cannot be completely averaged by spinning about one axis. Nolle [13] first reported the narrowing of the central transition of ^{95}Mo in $Mo(CO)_6$, upon sample rotation ($\nu_\mathrm{rot} = 60$ Hz) about an axis perpendicular to the static magnetic field and calculated the theoretical powder spectra for $\eta = 0$. The first MAS studies ($\nu_\mathrm{rot} = 2.6 - 5.0$ kHz) of half-integer nuclei were published in 1981 [14-16]. A numerical calculation of the narrowing factor $\sqrt{M_2/M_2^\mathrm{rot}}$ for the dependence of the second-order quadrupole-broadened center transition on the rotation angle was published by Dirk Müller [17] and is presented in Fig. 4.1. In can be seen that the angle of 65° gives the maximum line-narrowing factor of about 5, whereas the narrowing factor for the magic-angle $\theta_\mathrm{m} = \arccos 3^{-1/2} \approx 54.74°$ is only about 3.6; see Eq. (1.74).

Spinning at variable angles allows the determination of quadrupole parameters. Oldfield and co-workers [18, 19] established a variable-angle-spinning technique for quadrupolar nuclei. Acronyms are VAS NMR or VASS NMR. The powder average approaches of Alderman *et al.* [20] and Sethi *et al.* [21] for the computation of sideband intensities were extended by Zheng *et al*. [22] for spectra of the central transition of quadrupole nuclei with half-integer spin in powdered solids spinning at any angle and at any speed. Lefebvre *et al.* [23] neglected dipolar interactions and the anisotropy of the chemical shift, and concluded that the angle θ = 43.5° allows an easy determination of quadrupole parameters. The VAS NMR technique was used in about 20 studies between 1982 and 1998 for relatively "diluted" quadrupolar nuclei [24].

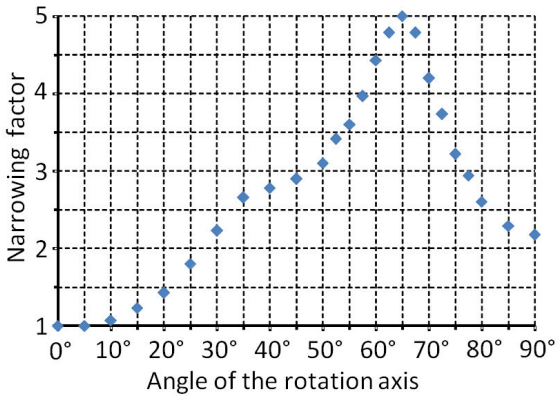

Fig. 4.1. Narrowing factor $\sqrt{M_2/M_2^{\mathrm{rot}}}$ for the second-order quadrupole-broadened centerband of the central transition for rotation about axes inclined at the given angle with respect to the direction of the external magnetic field. The values were calculated with respect to the center of gravity and without consideration of spinning sidebands for M_2^{rot} by Dirk Müller.

Although the second-order quadrupole shift is not completely averaged using MAS, working at the magic angle still has the advantage of removing effects due to dipole interactions and chemical shift anisotropy. Therefore, MAS line shape simulations of the central transition are more accurate than static powder spectra. It can be stated for all NMR interactions which cause a signal broadening much greater than the MAS frequency that a higher frequency yields better focusing of signal intensity to the remaining rotation sidebands. With respect to the quadrupole interaction in particular, the MAS frequency should be greater than the second-order quadrupole broadening of the central transition, and a rotation frequency of about 30 kHz is often necessary. The maximum rotation frequency depends on the diameter of the rotor [25]. Commercially available rotors reach 8 kHz for a 7-mm diameter, 18 kHz for 4 mm, 35 kHz for 2.5 mm, 80 kHz for 1 mm [26] and 110 kHz for 0.75 mm (JEOL NM 120001). But the smaller rotor diameter is connected with a smaller signal-to-noise ratio, since the signal intensity is proportional to the square of the sample diameter. We compared the ^{27}Al signal of a zeolite using different rotors, adjusted the length of the excitation pulse to the maximum signal amplitude and obtained the relative signal-to-noise ratios from experiments in a 7-mm-rotor with 100%, in the 4-mm-rotor with 37%, in the 2.5-mm-rotor with 12% and in the 1.6-mm-rotor with 6%. Correspondingly, a 0.7-mm-rotor would yield 1%.

Intensity measurements are not recommended for MAS when the spectrum consists of a single signal. But the quantification of MAS spectra is necessary if MAS is to allow different species to be distinguished. In principle, MAS does not affect the intensity, $G(0)$, as long as the duration of the pulse is short compared with the rotation cycle. But the spectral distribution of intensity changes and the intensities of the spinning sidebands have to be have to be added to the intensity of the centerband [27] if the MAS frequency is not larger than the width of the static spectrum.

For a small quadrupole coupling, some intensity from the satellite transitions appears in the zero-order spinning sideband. This so-called centerband of the satellite transitions overlaps the centerband of the central transition and has to be subtracted if the intensities of central transitions are compared. It can be neglected for strong quadrupole coupling, if we have for the quadrupole frequency $\nu_{\mathrm{Q}}(2I-1) > 100\ \nu_{\mathrm{rot}}$. The subtraction is not difficult, since the intensities of zero-order and first- or second-order spinning sidebands of the satellites show only a small difference for $\nu_{\mathrm{Q}}(2I-1) > 10\ \nu_{\mathrm{rot}}$.

However, for $(\nu_{\mathrm{Q}}^2/3\nu_{\mathrm{L}})[I(I+1)-3/4] > \nu_{\mathrm{rot}}$ the signal of the central transition also splits into a centerband and a few spinning sidebands. These central transition spinning sidebands must be added to the centerband to compare intensities. The addition procedure decreases the signal-to-noise ratio and multiplies the contribution from the satellite transitions.

4.2 Dynamic Angle Spinning (DAS)

As already shown in Chapter 1.4, the second-order quadrupole broadening of NMR signals can be described by Legendre polynomials of degree two and four. With ν_{cg} as the center of gravity of the line shape, F as a function of ν_L, ν_Q, η and I, and $A_l(\phi,\psi)$ as an angle-dependent contribution, where ϕ,ψ are Euler angles describing the transformation between the quadrupole PAS and the rotor axis, we obtain for the central transition

$$\nu - \nu_L = \nu_{cg} + \sum_{l=1;2} F\ A_l(\phi,\psi) P_l(\cos\beta). \tag{4.05}$$

The term $P_l(\cos\beta)$ depends on the Euler angle β, the rotor axis orientation with respect to the external field, and is given by the 2- and 4-degree Legendre polynomials:

$$P_2 = \tfrac{1}{2}(3\cos^2\beta - 1), \qquad P_4 = \tfrac{1}{8}(35\cos^4\beta - 30\cos^2\beta + 3). \tag{4.06}$$

The Legendre polynomials correspond to the values $m' = m = 0$ in the table of the reduced Wigner d-Matrix elements for rank $k = 2$ and 4. For $P_2 = 0$ it is inferred that $\beta = \arccos 3^{-1/2} \approx 54.74°$, which is the magic angle. This means that the first summand in Eq. (4.05) vanishes upon MAS. $P_4 = 0$ yields $\beta = \arccos\sqrt{\frac{3}{7} \pm \frac{2}{7}\sqrt{\frac{6}{5}}} \approx 30.56°$ or $70.12°$. Based on these considerations, double rotation (DOR) operates with two angles of rotation, $\beta_1 = 30.56°$ and $\beta_2 = 54.74°$, or alternatively, $\beta_1 = 70.12°$ and $\beta_2 = 54.74°$.

For dynamic angle spinning (DAS) we consider the phase development of the anisotropic part after two equal time periods of rotation around two sequenced angles, β_1 and β_2. A refocusing is obtained if two conditions are fulfilled: $P_2(\cos\beta_1) = -P_2(\cos\beta_2)$ and $P_4(\cos\beta_1) = -P_4(\cos\beta_2)$. It can be solved for $\beta_1 \approx 37.38°$ and $\beta_2 \approx 79.19°$. Different pairs of angles can be obtained by using unequal time periods for the angles. If one angle in the pair is set to the magic angle, no solution exists.

DAS experiments were first performed independently by Chmelka *et al.* [28] and Llor and Virlet [29]. The rotor axis toggles in the simple case between the two angles of 37.38° and 79.19° for two equal periods of time $t_1/2$. During the hopping time, necessary for switching the angle (ca. 30 ms), a minimization of the evolution of the magnetization can be achieved by means of two π/2 pulses at the beginning and at the end of the hopping time. The pulses must be selective and calibrated corresponding to the angle of rotation. The signal is the second-order quadrupole echo with a maximum at time t_1 after the last pulse. The data acquisition starts after the last pulse for the full echo observation and gives the data for the F_2 domain. A 2D spectrum can be acquired by varying t_1 for obtaining the F_1 domain.

There are four limitations to the application of the DAS technique. First, the spin-lattice relaxation time, T_1, often short for quadrupole nuclei, has to be larger than the time period necessary for the hopping of the rotor axis. Second, a strong homonuclear dipolar interaction is destructive for the second-order quadrupole echo. Third, the spin exchange due to dipolar interactions cannot be eliminated during the hopping time of the rotor axis, and has to be sufficiently small. Last but not least, a special probe is necessary for the angle hopping.

But many DAS NMR investigations on ^{17}O, ^{87}Rb and other nuclei have been successfully performed [30]. The Web of Science refers to 25 experimental DAS studies in the years 1988-2001, one DAS exchange experiment in 2004 [31] and, since this time, various reviews. A concluding review was presented by Grandinetti [30].

4.3 Double-Rotation (DOR)

Before 1988 only a few scientists believed in the possibility of building a rotor for double rotation, even though Eqs. (4.05) and (4.06) were well-known as the theoretical foundation for the cancellation of the second-order quadrupole broadening of NMR signals. But in that year Samoson *et al.* [32] succeeded in building a double-rotor probe. The outer rotor, inclined by $\beta_2 = 54.74°$ with respect to the external field, rotated at about 400 Hz, and had a diameter of 20 mm. The sample in the inner rotor, 5 mm diameter, rotated at about 2 kHz, and the angle between the two axes of rotation was $\beta_1 = 30.56°$ [32].

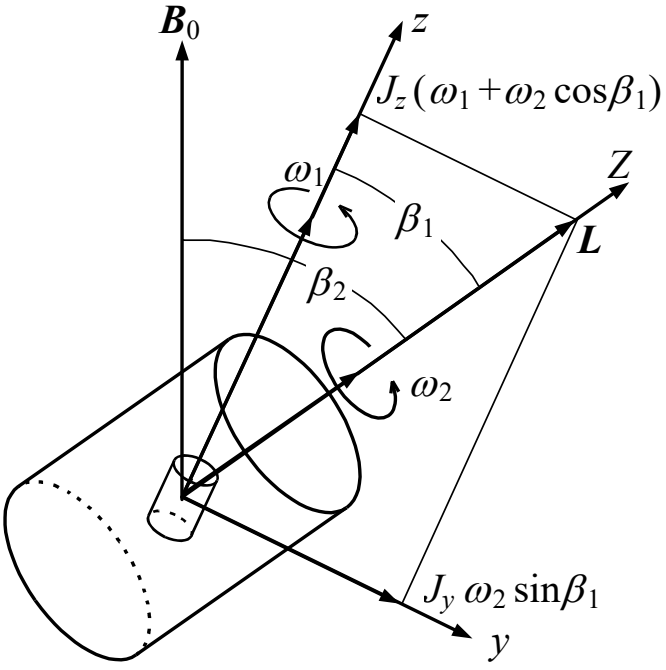

Fig. 4.2. Moments of inertia for double rotation. By adjusting the ratio of moments, J_y/J_x, the two added vector components of the angular momentum along the inner-rotor axis z and the y axis could be made to point along the outer-rotor axis Z, so that spinning the outer rotor would not affect the orientation of the total angular momentum of the inner rotor [33].

A torque-free rotation can be achieved only for a certain ratio of $k = \omega_1/\omega_2$. Two contributions to the inner-rotor angular velocity are the angular rotation within the inner rotor, ω_1, and the angular velocity ω_2 imposed by the outer rotor. The latter can be decomposed into one component $\omega_2 \cos\beta_1$ along the z-axis of the inner rotor, and another component $\omega_2 \sin\beta_1$ perpendicular to this axis in y-direction, so that the y -direction, axis z of the inner rotor, and axis Z of the outer rotor are all in one plane. Thus, $\omega_x = 0$, $\omega_y = \omega_2 \sin\beta_1$, $\omega_z = \omega_1 + \omega_2 \cos\beta_1$, and the resulting angular momentum L must be in the Z-direction in order to be torque-free [34]; see Fig. 4.2. The result is

$$\tan\beta_1 = \frac{J_y\,\omega_2 \sin\beta_1}{J_z(\,\omega_1 + \omega_2 \cos\beta_1)}\,. \tag{4.07}$$

For $\beta_1 = \arccos\sqrt{\frac{3}{7} + \frac{2}{7}\sqrt{\frac{6}{5}}} \approx 30.56°$, we obtain

$$\frac{\omega_1}{\omega_2} \equiv \frac{\nu_{\text{inner}}}{\nu_{\text{outer}}} = k \approx 0.861\left(\frac{J_y}{J_z} - 1\right), \tag{4.08}$$

and the usual design of the inner rotor gives values of J_y/J_z so that $5 < k < 6$. Wu *et al.* [34] explained that the spinning system is in a stable state when the torque-free condition. given by Eq. (4.08), is slightly violated and the frequencies obey the equation

$$\nu_{\text{inner}} = k\,\nu_{\text{outer}} + \Delta\,\nu_{\text{inner}}, \tag{4.09}$$

where the excess of the inner frequency, $\Delta\,\nu_{\mathrm{inner}}$, is about 1 kHz.

DOR NMR gives accurate values of the isotropic shift, δ_{iso}, of the nuclear magnetic resonance of a quadrupole nucleus. Two shift effects are superimposed, the isotropic quadrupole shift (see Eq. (1.69)) and the isotropic contribution of the chemical shift (see Eq. (1.95)). We replace the isotropic part of the shielding tensor, σ_{iso}, with the isotropic chemical shift

$$\delta_{\mathrm{CS\,iso}} = \sigma_{\mathrm{ref}} - \sigma_{\mathrm{iso}}, \tag{4.10}$$

where σ_{ref} denotes the isotropic shielding of a reference compound. Conventionally, in the determination of the gyromagnetic ratio, γ, the reference compound yields a signal at $\nu_{\mathrm{L}} = B_0\gamma/2\pi$ [35]. This means that $\sigma_{\mathrm{ref}} = 0$, if we take into consideration that the shielding, introduced in Eq. (1.95) as a dimensionless factor of B_0, is like the chemical shift values usually expressed in the relative units 'parts per million', ppm, with respect to the Larmor frequency. We substitute the isotropic part of the second-order quadrupole shift $\nu_{-1/2,1/2} - \nu_{\mathrm{L}}$ in Eq. (1.69) by the ppm-units $\delta_{\mathrm{Q\,iso}} = 10^6\left(\nu_{-1/2,1/2} - \nu_{\mathrm{L}}\right)/\nu_{\mathrm{L}}$. In this notation we obtain for the observed isotropic shift in the DOR experiment

$$\delta_{\mathrm{DOR}} = \delta_{\mathrm{iso}} = \delta_{\mathrm{CS\,iso}} + \delta_{\mathrm{Q\,iso}} = \delta_{\mathrm{CS\,iso}} - \frac{10^6\nu_{\mathrm{Q}}^2}{30\,\nu_{\mathrm{L}}^2}\left[I(I+1) - \frac{3}{4}\right]\left(1 + \frac{\eta^2}{3}\right). \tag{4.11}$$

The equation reflects the fact that the quadrupole shift decreases quadratically with increasing external field ($B_0 = 2\pi\nu_{\mathrm{L}}/\gamma$). We see that the value of the isotropic chemical shift cannot be obtained from a single DOR experiment. Two DOR experiments at different Larmor frequencies could be applied, in order to obtain chemical and quadrupole shifts. But the easier option is the determination of the quadrupole parameter by the simulation of an additional measured MAS spectrum.

The analysis of the DOR sidebands can give additional information [36-38]. But the application of rotation-synchronized pulses has been shown to be effective in eliminating half of the DOR sidebands [39], if they are undesirable. Total suppression of the sidebands can be achieved by the application of additional pulses [40, 41]. DOR has been combined with cross-polarization [42], with two-dimensional homonuclear correlation experiments [43, 44], with double-quantum coherences in homonuclear spin systems [45] and with the multiple-quantum technique [46-49]. A recent review was presented by Dupree [50].

The rotation frequencies of the inner and outer rotor presently do not exceed ν_{inner} = 12 kHz and ν_{outer} = 2 kHz, respectively. A pneumatic unit, which is controlled by a computer, simplifies the experimental set-up and makes it safer. Compared to the MAS technique, a more complicated set-up and stronger wear of the rotors must be accepted for DOR experiments. The filling factor of the RF coil is low, since the sample is located in the smaller inner rotor. Nevertheless, the DOR NMR spectra exhibit a relatively good signal-to-noise ratio, since the signals are relatively narrow. A comparison of the signal-to-noise ratios of ^{27}Al NMR spectra of andalusite in the external field of 17.6 T showed the values 555, 615 and 197 for the MAS spectrum, DOR spectrum and 3QMAS DFS spectrum, respectively [51].

The Web of Science refers to about 200 DOR studies in the years 1988-2012, among them about 40 studies with Ago Samoson as one of the authors. About 130 papers were published before 2000, and about 30 papers have come out more recently, in the years 2009-2012. The fact that DOR probes are not commercially available at present probably limits the use of DOR.

4.4 MAS Spectra of Spin-1/2 Nuclei Coupled to Quadrupolar Nuclei

The title of the given review "Quadrupole Effects in Solid-State NMR" involves the well-known effect that MAS fails to completely eliminate the effect of dipolar coupling for spin-1/2 nuclei when coupled to quadrupole nuclei with a quadrupole frequency comparable to the Zeeman frequency of the quadrupolar nuclei. This phenomenon was first discovered for the spin-1/2-spin-1 pair ^{13}C-^{14}N by Opella et al. [52]. Reviews were presented by R.K. Harris [53, 54] and Olivieri [55, 56]. The spin-1/2 spectra, calculated by using first-order perturbation theory, show for the individual values of m the typical quadrupole second-order line shape [57]. The transmitted influence can be described as the second-order quadrupole effect on NMR spectra of spin-1/2 nuclei [58] which is on the ppm-scale with respect to the external field, B_0, proportional to $1/B_0^2$.

Olivieri [57] estimated the narrowing effect by MAS and calculated $\nu_{m\,\mathrm{iso}}$, the isotropic shift of the line ν_m of one resonant spin-1/2, dipolar coupled to one quadrupole nucleus in the state m (first-order pertubative approach, spatial averaging for powder samples, and fast sample spinning so that spinning sidebands do not overlap with the center band). In our notation, it is

$$\nu_{m\,\mathrm{iso}} = \frac{\Delta\nu_{\mathrm{IS}}\,\nu_{\mathrm{Q}}}{10\,\nu_{\mathrm{S}}}[S(S+1)-3m^2](3\cos^2\beta - 1 + \eta\sin^2\beta\cos 2\alpha) \tag{4.12}$$

with the dipolar splitting

$$\Delta\nu_{\mathrm{IS}} = \frac{\mu_0}{4\pi}\frac{\gamma_{\mathrm{I}}\gamma_{\mathrm{S}}\,h}{4\pi^2}\,\frac{1}{r_{ik}^3} \tag{4.13}$$

and the quadrupole frequency, cf. Eq. (1.50),

$$\nu_{\mathrm{Q}} = \frac{3e^2qQ}{2S(2S-1)h}. \tag{4.14}$$

The dipolar splitting, $\Delta\nu_{\mathrm{IS}}$, is the frequency distance between singularities of the inner Pake's doublet of the static powder spectrum of an $I-S$ spin pair of distance r_{ik}. The quadrupole frequency, ν_{Q}, of the non-resonant S-spins is defined by Eq. (4.14). The Larmor frequency of the non-resonant quadrupole nucleus is ν_{S}, η is the asymmetry parameter, and the angles β and α define the orientation of the vector connecting the spin pair in the PAS of the quadrupole interaction; see Sect. 1.4. The shift can be positive or negative, or even disappear for the hypothetical case of $\beta = \arccos\left(1/\sqrt{3}\right)$ and $\eta = 0$. The geometry factor in the round brackets of Eq. (4.12) is 2 if the dipolar and quadrupolar principle axis systems are coincident ($\beta = 0$).

An estimate of the line narrowing by MAS, is given by the narrowing factor $(M_2^{\text{Van Vleck}}/M_2^{\mathrm{MAS}})^{1/2}$. Van Vleck's second moment for a heteronuclear spin pair (powder) can be obtained from Eqs. (4.13) and (1.84) in squared frequency units as

$$M_2^{\text{Van Vleck}} = \frac{4}{15}\Delta\nu_{\mathrm{IS}}^2\,S(S+1). \tag{4.15}$$

If only quadrupole effects are present, spinning sidebands are not considered, and ν_{Q} is extremely small, M_2^{MAS} vanishes. For a stronger quadrupole interaction M_2^{MAS} can be calculated by summing up the values of $\nu_{m\,\mathrm{iso}}$, given by Eq. (4.12):

$$M_2^{\text{MAS iso}} = \frac{1}{2S+1}\sum_{m=-S}^{m=+S} \nu_{m\,\text{iso}}^2$$

$$= M_2^{\text{Van Vleck}} \frac{\nu_\text{Q}^2}{\nu_\text{S}^2}\frac{3}{400}(2S-1)(2S+3)(3\cos^2\beta - 1 + \eta\sin^2\beta\cos 2\alpha)^2. \qquad (4.16)$$

Fenzke [59] calculated both the isotropic and the anisotropic contributions to the second moment and obtained

$$M_2^{\text{MAS iso+aniso}} = \frac{1}{2S+1}\sum_{m=-S}^{m=+S} \nu_{m\,\text{iso}}^2$$

$$= M_2^{\text{Van Vleck}} \frac{\nu_\text{Q}^2}{\nu_\text{S}^2}\frac{3}{400}(2S-1)(2S+3) \qquad (4.17)$$

$$\times\left[\frac{730}{729}(3\cos^2\beta - 1 + \eta\sin^2\beta\cos 2\alpha)^2 + \frac{20}{729}(4 + 3\cos^2\beta + 2\eta^2 - \eta^2\cos^2\beta - 2\eta\sin^2\beta\cos 2\alpha)\right].$$

Eq. (4.17) shows that the main contribution to $M_2^{\text{MAS iso+aniso}}$ arises from the isotropic part, except when the angle between both nuclei and the z-axis of the field gradient tensor is the magic angle. From Eqs. (4.15) and (4.17), the narrowing factor can be obtained as a function of β, α and S. The analytically obtained values agree with the numerically calculated values of Böhm et al. [60] for $S = 3/2$ and $S = 5/2$ in the case of $\nu_\text{Q} < \nu_\text{S}$. For $\nu_\text{Q} \geq \nu_\text{S}$, the perturbative approach cannot be applied. Böhm et al. [60] showed that for $\nu_\text{Q} > \nu_\text{S}$ there is only a small difference between M_2^{MAS} and $M_2^{\text{Van Vleck}}$.

For coincident dipolar and quadrupolar principle axis systems and $\nu_\text{Q} < \nu_\text{S}$, the narrowing factor can be approximated with an error of less than 15% by

$$\sqrt{\frac{M_2^{\text{Van Vleck}}}{M_2^{\text{MAS}}}} \approx \frac{5\nu_\text{S}}{2S\nu_\text{Q}}. \qquad (4.18)$$

Recent studies of Lu et al. [61, 62] concern the inter-nuclear distance measurement between spin-1/2 and quadrupolar nuclei and propose appropriate heteronuclear dipolar recoupling methods.

4.5 References

[1] E.R. Andrew, A. Bradbury, R.G. Eades, NMR Spectra from a Crystal Rotated at High Speed, Nature 182 (1958) 1659-1659. https://doi.org/10.1038/1821659a0.

[2] E.R. Andrew, Magic Angle Spinning in Solid State NMR Spectroscopy, Phil. Trans. R. Soc. Lond. A 299 (1981) 505-520. https://doi.org/10.1098/rsta.1981.0032.

[3] Z.H. Gan, Isotropic NMR Spectra of Half-integer Quadrupolar Nuclei Using Satellite Transitions and Magic-angle Spinning, J. Am. Chem. Soc. 122 (2000) 3242-3243. https://doi.org/10.1021/ja9939791.

[4] Z. Gan, Satellite Transition NMR Spectroscopy of Half-Integer Quadrupolar Nuclei under Magic-Angle Spinning, in: eMagRes, John Wiley & Sons, Ltd, 2007. https://doi.org/10.1002/9780470034590.emrstm0481.

[5] S.E. Ashbrook, S. Wimperis, STMAS NMR: Experimental Advances, in: R.E. Wasylishen, S.E. Ashbrook, S. Wimperis (Eds.) NMR of Quadrupolar Nuclei in Solid Materials, Wiley, Chichester, 2012, pp. 163-178.

[6] S. Mamone, A. Dorsch, O.G. Johannessen, M.V. Naik, P.K. Madhu, M.H. Levitt, A Hall Effect Angle Detector for Solid-state NMR, J. Magn. Reson. 190 (2008) 135-141. https://doi.org/10.1016/j.jmr.2007.07.012.

[7] J. Herzfeld, A.E. Berger, Sideband Intensities in NMR Spectra of Samples Spinning at the Magic Angle, J. Chem. Phys. 73 (1980) 6021-6030. https://doi.org/10.1063/1.440136.

[8] J.S. Frye, G.E. Maciel, Setting the Magic-angle Using a Quadrupolar Nuclide, J. Magn. Reson. 48 (1982) 125-131. https://doi.org/10.1016/0022-2364(82)90243-8.

[9] J. Skibsted, N.C. Nielsen, H. Bildsöe, H.J. Jacobsen, Satellite Transitions in MAS NMR Spectra of Quadrupolar Nuclei, J. Magn. Reson. 95 (1991) 88-117. https://doi.org/10.1016/0022-2364(91)90327-P.

[10] H.J. Jakobsen, A.R. Hove, H. Bildsoe, J. Skibsted, Satellite Transitions in Natural Abundance Solid-state ^{33}S MAS NMR of Alums - Sign Change with Zero-crossing of C_Q in a Variable Temperature Study, J. Magn. Reson. 180 (2006) 170-177. https://doi.org/10.1016/j.jmr.2006.02.006.

[11] U.G. Nielsen, A. Hazell, J. Skibsted, H.J. Jakobsen, C.J. McKenzie, Solid-state ^{51}V MAS NMR Spectroscopy Determines Component Concentration and Crystal Phase in Co-crystallised Mixtures of Vanadium Complexes, CrystEngComm 12 (2010) 2826-2834. https://doi.org/10.1039/b922687g.

[12] H.J. Jakobsen, H. Bildsoe, Z. Can, W.W. Brey, Experimental Aspects in Acquisition of Wide Bandwidth Solid-state MAS NMR Spectra of Low-γ Nuclei with Different Opportunities on Two Commercial NMR Spectrometers, J. Magn. Reson. 211 (2011) 195-206. https://doi.org/10.1016/j.jmr.2011.05.015.

[13] A. Nolle, Second-order Quadrupole Splittings of the ^{95}Mo NMR Signal in $MO(CO)_6$ and their Reduction by Sample Spinning, Z. Physik A 280 (1977) 231-234. https://doi.org/10.1007/BF01434345.

[14] D. Freude, H.-J. Behrens, Investigation of ^{27}Al NMR Chemical Shifts in Zeolites of the Faujasite Type, Cryst. Res. Technol. 16 (1981) K36-K38. https://doi.org/10.1002/crat.19810160322.

[15] D. Müller, W. Gessner, H.J. Behrens, G. Scheler, Determination of the Aluminum Coordination in Aluminum-oxygen Compounds by Solid-state High-resolution ^{27}Al NMR, Chem. Phys. Lett. 79 (1981) 59-62. https://doi.org/10.1016/0009-2614(81)85288-8.

[16] E. Kundla, A. Samoson, E. Lippmaa, High-resolution NMR of Quadrupolar Nuclei in Rotating Solids, Chem. Phys. Lett. 83 (1981) 229. https://doi.org/10.1016/0009-2614(81)85451-6.

[17] D. Freude, NMR Investigations of Proton Donator and Electron Acceptor Properties in Heterogeneous Systems, Adv. Colloid Interface Sci. 23 (1985) 21-43. https://doi.org/10.1016/0001-8686(85)80015-4.

[18] S. Ganapathy, S. Schramm, E. Oldfield, Variable-Angle Sample-Spinning High Resolution NMR of Solids, J. Chem. Phys. 77 (1982) 4360-4365. https://doi.org/10.1063/1.444436.

[19] E. Oldfield, S. Schramm, M.D. Meadows, K.A. Smith, R.A. Kinsey, J. Ackerman, High-resolution NMR spectroscopy of quadrupolar nuclei in solids: Sodium salts, J. Am. Chem. Soc. 104 (1982) 919-920. https://doi.org/10.1021/ja00367a074.

[20] D.W. Alderman, M.S. Solum, D.M. Grant, Methods for Analyzing Spectroscopic Line Shapes. NMR Solid Powder Pattern, J. Chem. Phys. 84 (1986) 3717-3725. https://doi.org/10.1063/1.450211.

[21] N.K. Sethi, D.W. Alderman, D.M. Grant, NMR-spectra from Powdered Solids Spinning at Any Angle and Speed - Simulations and Experiments, Mol. Phys. 71 (1990) 217-238. https://doi.org/10.1080/00268979000101761.

[22] Z.W. Zheng, Z.H. Gan, N.K. Sethi, D.W. Alderman, D.M. Grant, An Efficient Simulation of Variable-angle Spinning Lineshapes for the Quadrupolar Nuclei with Half-integer Spin, J. Magn. Reson. 95 (1991) 509-522. https://doi.org/10.1016/0022-2364(91)90165-P.

[23] F. Lefebvre, J.P. Amoureux, C. Fernandez, E.G. Derouane, Investigation of Variable Angle Sample Spinning (VASS) NMR of Quadrupolar Nuclei. 1. Theory., J. Chem. Phys. 86 (1987) 6070-6076. https://doi.org/10.1063/1.452446.

[24] Z. Xu, J.F. Stebbins, Oxygen Sites in the Zeolite Stilbite: A Comparison of Static, MAS, VAS, DAS and Triple Quantum MAS NMR Techniques, Solid State Nucl. Magn. Reson. 11 (1998) 243-251. https://doi.org/0.1016/s0926-2040(97)00019-2.

[25] A. Samoson, T. Tuherm, J. Past, A. Reinhold, T. Anupold, N. Heinmaa, New Horizons for Magic-angle Spinning NMR, Top. Curr. Chem. 246 (2005) 15-31. https://doi.org/10.1007/b98647.

[26] Y. Nishiyama, Y. Endo, T. Nemoto, H. Utsumi, K. Yamauchi, K. Hioka, T. Asakura, Very Fast Magic Angle Spinning ^{1}H-^{14}N-2D Solid-state NMR: Sub-micro-liter Sample Data Collection in a Few Minutes, J. Magn. Reson. 208 (2011) 44-48. https://doi.org/10.1016/j.jmr.2010.10.001.

[27] M.M. Maricq, J.S. Waugh, NMR in Rotating Solids, J. Chem. Phys. 70 (1979) 3300-3316. https://doi.org/10.1063/1.437915

[28] B.F. Chmelka, K.T. Mueller, A. Pines, J. Stebbins, Y. Wu, J.W. Zwanziger, Oxygen-17 NMR in Solids by Dynamic-Angle Spinning and Double Rotation, Nature 339 (1989) 42-43. https://doi.org/10.1038/339042a0.

[29] A. Llor, J. Virlet, Towards high-resolution NMR of more nuclei in solids: Sample spinning with time-dependent spinner axis angle, Chem. Phys. Lett. 152 (1988) 248-253. https://doi.org/10.1016/0009-2614(88)87362-7.

[30] P.l. Grandinetti, Dynamic Angle Spinning, in: R.E. Wasylishen, S.E. Ashbrook, S. Wimperis (Eds.) NMR of Quadrupolar Nuclei in Solid Materials, Wiley, Chichester, 2012, pp. 121-132.

[31] T.G. Ajithkumar, E.R.H. van Eck, A.P.M. Kentgens, Homonuclear Correlation Experiments for Quadrupolar Nuclei, Spinning Away from the Magic-angle, Solid State Nucl. Magn. Reson. 26 (2004) 180-186. https://doi.org/10.1016/j.ssnmr.2004.03.005.

[32] A. Samoson, E. Lippmaa, A. Pines, High-resolution Solid-state NMR Averaging of Second-order Effects by means of a Double-rotor, Mol. Phys. 65 (1988) 1013-1018. https://doi.org/10.1080/00268978800101571.

[33] D. Freude, Quadrupole Nuclei in Solid-state NMR, in: R.A. Meyers (Ed.) Encyclopedia of Analytical Chemistry, John Wiley & Sons, Chichester, 2000, pp. 12188-12224. https://doi.org/10.1002/9780470027318.a6112.

[34] Y. Wu, B.Q. Sun, A. Pines, A. Samoson, E. Lippmaa, NMR Experiments with a New Double Rotor, J. Magn. Reson. 89 (1990) 297-309. https://doi.org/10.1016/0022-2364(90)90236-3.

[35] R.K. Harris, E.D. Becker, S.M.C. De Menezes, R. Goodfellow, P. Granger, NMR Nomenclature. Nuclear Spin Properties and Conventions for Chemical Shifts - (IUPAC Recommendations 2001), Pure Appl. Chem. 73 (2001) 1795-1818. https://doi.org/10.1351/pac200173111795.

[36] B.Q. Sun, J.H. Baltisberger, Y. Wu, A. Samoson, A. Pines, Sidebands in Dynamic Angle Spinning (DAS) and Double Rotation (DOR) NMR, Solid State Nucl. Magn. Reson. 1 (1992) 267-295. https://doi.org/10.1016/0926-2040(92)90047-D.

[37] E. Cochon, J.P. Amoureux, Sideband Analysis in DOR NMR Spectra. 1. 'Infinite' Inner-Rotor Speed, Solid State Nucl. Magn. Reson. 2 (1993) 205-222. https://doi.org/10.1016/0926-2040(93)90001-4.

[38] J.P. Amoureux, E. Cochon, Sideband Analysis in DOR NMR Spectra. 2. Real Finite Inner-rotor Speed, Solid State Nucl. Magn. Reson. 2 (1993) 223-234. https://doi.org/10.1016/0926-2040(93)90002-5.

[39] A. Samoson, E. Lippmaa, Synchronized Double-rotation NMR Spectrosocpy, J. Magn. Reson. 84 (1989) 410-416. https://doi.org/10.1016/0022-2364(89)90389-2.

[40] A. Samoson, J. Tegenfeldt, Suppression of DOR Sidebands, J. Magn. Reson. A 110 (1994) 238-244. https://doi.org/10.1006/jmra.1994.1210.

[41] F.A. Perras, D.L. Bryce, Removal of sidebands in double-rotation NMR in real time, Journal of Magnetic Resonance 211 (2011) 234-239. https://doi.org/10.1016/j.jmr.2011.05.002.

[42] Y. Wu, D. Lewis, J.S. Frye, A.R. Palmer, R.A. Wind., Cross-polarization Double-rotation NMR, J. Magn. Reson. 100 (1992) 425-430. https://doi.org/10.1016/0022-2364(92)90277-E.

[43] A.P.M. Kentgens, E.R.H. van Eck, T.G. Ajithkumar, T. Anupold, J. Past, A. Reinhold, A. Samoson, New Opportunities for Double Rotation NMR of Half-integer Quadrupolar Nuclei, J. Magn. Reson. 178 (2006) 212-219. https://doi.org/10.1016/j.jmr.2005.09.014.

[44] I. Hung, A.P. Howes, T. Anupold, A. Samoson, D. Massiot, M.E. Smith, S.P. Brown, R. Dupree, ^{27}Al Double Rotation Two-dimensional Spin Diffusion NMR: Complete Unambiguous Assignment of Aluminium Sites in $9Al_2O_3$ $2B_2O^3$, Chem. Phys. Lett. 432 (2006) 152-156. https://doi.org/10.1016/j.cplett.2006.10.085.

[45] A. Brinkmann, A.P.M. Kentgens, T. Anupold, A. Samoson, Symmetry-based Recoupling in Double-rotation NMR Spectroscopy, J. Chem. Phys. 129 (2008) 174507. https://doi.org/10.1063/1.3005395.

[46] A. Samoson, Two-Dimensional Isotropic NMR of Quadrupole Nuclei in Solids, J. Magn. Reson. 121 (1996) 209-211. https://doi.org/10.1006/jmra.1996.0163.

[47] A. Samoson, T. Anupold, Synchronized Double Rotation 2D NMR, Solid State Nucl. Magn. Reson. 15 (2000) 217-225. https://doi.org/10.1016/s0926-2040(99)00060-0.

[48] I. Hung, A. Wong, A.P. Howes, T. Anupold, A. Samoson, M.E. Smith, D. Holland, S.P. Brown, R. Dupree, Separation of Isotropic Chemical and Second-order Quadrupolar Shifts by Multiple-quantum Double Rotation NMR, J. Magn. Reson. 197 (2009) 229-236. https://doi.org/10.1016/j.jmr.2009.01.005.

[49] I. Hung, A.P. Howes, B.G. Parkinson, T. Anupold, A. Samoson, S.P. Brown, P.F. Harrison, D. Holland, R. Dupree, Determination of the Bond-angle Distribution in Vitreous B_2O_3 by B-11 Double Rotation (DOR) NMR spectroscopy, J. Solid State Chem. 182 (2009) 2402-2408. https://doi.org/10.1016/j.jssc.2009.06.025.

[50] R. Dupree, Double Rotation (DOR) NMR, in: R.E. Wasylishen, S.E. Ashbrook, S. Wimperis (Eds.) NMR of Quadrupolar Nuclei in Solid Materials, Wiley, Chichester, 2012, pp. 133-142.

[51] J. Kanellopoulos, D. Freude, A. Kentgens, A Practical Comparison of MQMAS Techniques, Solid State Nucl. Magn. Reson. 32 (2007) 99-108. https://doi.org/10.1016/j.ssnmr.2007.09.003.

[52] S.J. Opella, M.H. Frey, T.A. Cross, Detection of Individual Carbon Resonances in Solid Proteins, J. Am. Chem. Soc. 101 (1979) 5856-5857. https://doi.org/10.1021/ja00513a080.

[53] R.K. Harris, Magic Angle Spinning: Effects of Quadrupolar Nuclei on Spin-1/2 Spectra, in: eMagRes, John Wiley & Sons, Ltd, 2007. https://doi.org/10.1002/9780470034590.emrstm0285.

[54] R.H. Harris, Magic Angle Spinning: Effects of Quadrupolar Nuclei on Spin-1/2 Spectra, in: D.M. Gran, R.K. Harris (Eds.) Encyclopedia of Nuclear Magnetic Resonance, Wiley, Chichester, 1996, pp. 2909-2914.

[55] A.C. Olivieri, Solid State NMR Using Quadrupolar Nuclei, in: L. Editor-in-Chief: John (Ed.) Encyclopedia of Spectroscopy and Spectrometry (Second Edition), Academic Press, Oxford, 2010, pp. 2577-2586. https://doi.org/http://dx.doi.org/10.1016/B978-0-12-374413-5.00286-4.

[56] A.C. Olivieri, Solid-State NMR Using Quadrupolar Nuclei, in: C.L. Editor-in-Chief: John (Ed.) Encyclopedia of Spectroscopy and Spectrometry, Elsevier, Oxford, 1999, pp. 2116-2127. https://doi.org/http://dx.doi.org/10.1006/rwsp.2000.0283.

[57] A.C. Olivieri, Quadrupolar Effects in the CPMAS NMR Spectra of Spin-1/2 Nuclei, J. Magn. Reson. 81 (1989) 201-205. https://doi.org/10.1016/0022-2364(89)90281-3.

[58] R. Gobetto, R.K. Harris, D.C. Apperley, Second-order Quadrupolar Effects on NMR Spectra of Spin-1/2 Nuclei in Solids, Transmitted by Dipolar Coupling. ^{31}P(1/2) to ^{55}Mn(S=5/2), ^{59}Co(S=7/2), ^{93}Nb(S=9/2), J. Magn. Reson. 96 (1992) 119-130. https://doi.org/10.1016/0022-2364(92)90291-E.

[59] D. Fenzke, Equation for isotropic and anisotropic contributions to the MAS second moment for spin-1/2 nuclei upon dipolar interaction to quadrupolar nuclei, personal communication, 1992.

[60] J. Böhm, D. Fenzke, H. Pfeifer, Effects of Quadrupolar Nuclei on NMR Spectra of *I*=1/2 Nuclei in Magic-angle Spinning Experiments, J. Magn. Reson. 55 (1983) 197-204. https://doi.org/10.1016/0022-2364(83)90232-9.

[61] X. Lu, O. Lafon, J. Trebosc, J.-P. Amoureux, Detailed Analysis of the S-RESPDOR Solid-state NMR Method for Inter-nuclear Distance Measurement Between Spin-1/2 and Quadrupolar Nuclei, J. Magn. Reson. 215 (2012) 34-49. https://doi.org/10.1016/j.jmr.2011.12.009.

[62] X. Lu, O. Lafon, J. Trebosc, G. Tricot, L. Delevoye, F. Mear, L. Montagne, J.P. Amoureux, Observation of Proximities Between Spin-1/2 and Quadrupolar Nuclei: Which Heteronuclear Dipolar Recoupling Method is Preferable?, J. Chem. Phys. 137 (2012) 144201. https://doi.org/10.1063/1.4753987.